

# Pathways of DNA Double-Strand Break Repair during the Mammalian Cell Cycle

Kai Rothkamm,<sup>1</sup> Ines Krüger,<sup>1</sup> Larry H. Thompson,<sup>2</sup> and Markus Löbrich<sup>1\*</sup>

*Fachrichtung Biophysik, Universität des Saarlandes, D-66421 Homburg/Saar, Germany,<sup>1</sup> and Biology and Biotechnology Research Program, Lawrence Livermore National Laboratory, Livermore, California 94550<sup>2</sup>*

Received 26 December 2002/Returned for modification 9 May 2003/Accepted 16 May 2003

**Little is known about the quantitative contributions of nonhomologous end joining (NHEJ) and homologous recombination (HR) to DNA double-strand break (DSB) repair in different cell cycle phases after physiologically relevant doses of ionizing radiation. Using immunofluorescence detection of  $\gamma$ -H2AX nuclear foci as a novel approach for monitoring the repair of DSBs, we show here that NHEJ-defective hamster cells (CHO mutant V3 cells) have strongly reduced repair in all cell cycle phases after 1 Gy of irradiation. In contrast, HR-defective CHO irs1SF cells have a minor repair defect in G<sub>1</sub>, greater impairment in S, and a substantial defect in late S/G<sub>2</sub>. Furthermore, the radiosensitivity of irs1SF cells is slight in G<sub>1</sub> but dramatically higher in late S/G<sub>2</sub>, while V3 cells show high sensitivity throughout the cell cycle. These findings show that NHEJ is important in all cell cycle phases, while HR is particularly important in late S/G<sub>2</sub>, where both pathways contribute to repair and radioresistance. In contrast to DSBs produced by ionizing radiation, DSBs produced by the replication inhibitor aphidicolin are repaired entirely by HR. irs1SF, but not V3, cells show hypersensitivity to aphidicolin treatment. These data provide the first evaluation of the cell cycle-specific contributions of NHEJ and HR to the repair of radiation-induced versus replication-associated DSBs.**

DNA double-strand breaks (DSBs) are considered the most biologically damaging lesions produced by ionizing radiation (IR) and some chemicals. They also arise endogenously during DNA replication or as initiators of programmed processes, such as V(D)J recombination and meiotic exchange. If left unrepaired, DSBs can result in permanent cell cycle arrest, induction of apoptosis, or mitotic cell death caused by loss of genomic material (37); if repaired incorrectly, they can lead to carcinogenesis through translocations, inversions, or deletions (21, 67). Higher eukaryotic cells primarily repair DSBs by one of two genetically separable pathways, nonhomologous end joining (NHEJ) and homologous recombination (HR). NHEJ repairs broken ends with little or no requirement for sequence homology and involves the XRCC4-LIG4 complex and the DNA-dependent protein kinase (DNA-PK) holoenzyme, consisting of the DNA end-binding heterodimer Ku70-Ku80 and the catalytic subunit DNA-PK<sub>cs</sub> (22, 23, 53). Cell lines defective in any of these genes are generally highly IR sensitive ( $\leq 7$ -fold) and have marked deficiencies in DSB repair (9, 28, 40, 69).

HR, which appears to be less important than NHEJ for repairing IR-induced breaks in higher eukaryotes, utilizes extensive homology to faithfully restore the sequence at the break site by processes that involve proteins of the Rad52 epistasis group (20, 61, 62, 63). In human cells, the main steps in HR are thought to be mediated by the single-strand binding protein RPA (3, 18, 52); the human homologs of *Saccharomyces cerevisiae* Rad51, Rad52, and Rad54 (4, 56, 66); and the Rad51 paralogs XRCC2, XRCC3, Rad51B, Rad51C, and

Rad51D (reviewed in references 61, 62, 63, and 64). Evidence for a role of HR in the radioresistance of higher eukaryotes is derived from cell survival experiments with HR-defective mutants. While the disruption of Rad52 confers no sensitization (44, 73), inactivation of Rad54 causes a modest increase in radiosensitivity ( $\sim 1.7$ -fold in mouse embryonic stem cells) that is mainly associated with the late-S/G<sub>2</sub> phase (5, 15, 16, 57). The disruption of Rad51 is lethal (30, 54), but mutations in the Rad51 paralogs XRCC2 and XRCC3 confer significant radiosensitivity (11, 32, 58). The relatively high radioresistance of NHEJ-defective mutants in the late-S/G<sub>2</sub> portion of the cell cycle further suggests that HR promotes survival when sister chromatids are present (55, 72). A role for HR in DSB repair is also indirectly supported by cytogenetic investigations in which, for example, XRCC2- and XRCC3-defective hamster cells show highly elevated levels of spontaneous and IR-induced chromosomal aberrations (8, 17, 32, 59, 65). Additionally, homology-directed repair of I-SceI-produced site-specific DSBs depends strongly on XRCC2 and XRCC3 in hamster cells (24, 38) and, to a lesser extent, on Rad54 in mouse embryonic stem cells (14). These HR events primarily involve sister chromatids as a template for repair, resulting in gene conversion and not reciprocal exchange (25).

However, investigations with pulsed-field gel electrophoresis (PFGE) or similar approaches that directly quantify DSB repair by determining the molecular weights of broken DNA molecules have not detected a significant role of HR in the repair of radiation-induced DSBs. In these assays, in which IR doses of  $\geq 20$  Gy are used, unsynchronized XRCC2- and XRCC3-defective rodent cells show repair kinetics similar to those of wild-type cells (2, 10, 17, 26, 60). Similar findings have been obtained with HR mutants of DT40 chicken cells (70; K. Rothkamm and M. Löbrich, unpublished data).

The induction and repair of individual IR-induced DSBs in

\* Corresponding author. Mailing address: Fachrichtung Biophysik, Universität des Saarlandes, D-66421 Homburg/Saar, Germany. Phone: 49-6841-1626202. Fax: 49-6841-1626160. E-mail: markus.loebrich@uniklinik-saarland.de.

confluent primary human fibroblasts were recently investigated by enumeration of  $\gamma$ -H2AX foci (phosphorylated histone H2AX [45]) and by PFGE (49). When a fluorescent antibody specific for  $\gamma$ -H2AX was used, the discrete nuclear foci observed 3 min following irradiation numerically corresponded to the number of IR-induced DSBs determined in parallel by PFGE at much higher IR doses. Examination of the DSB repair-deficient cell line 180BR, which carries a defect in DNA ligase IV (40), further showed that the sealing of DSBs coincided temporally with the dephosphorylation of  $\gamma$ -H2AX. These results suggest that  $\gamma$ -H2AX foci can be used as an end point to measure the repair of radiation-induced DSBs at physiologically relevant doses.

In the present work, we used  $\gamma$ -H2AX foci to detect the presence of individual IR-induced DSBs (46) and thereby quantify the contributions of NHEJ and HR to DSB repair, based on mutant phenotypes. We show that NHEJ is important for IR-induced DSB repair in all cell cycle phases, whereas the role of HR is most critical in late S/G<sub>2</sub>. In contrast to DSBs produced by IR, DSBs generated during replication by aphidicolin treatment are repaired only by HR. These data provide the first cell cycle-specific evaluation of the contributions of NHEJ and HR to DSB repair after a radiation dose (1 Gy) which most wild-type cells can survive.

#### MATERIALS AND METHODS

**Cell growth and irradiation.** Chinese hamster ovary cells (K1, AA8, xrs-6, V3, V3-147, V3-155, irs1SF, and CXR3) were grown in minimum essential medium supplemented with 10% fetal bovine serum and antibiotics. All incubations were performed at 37°C in a humidified atmosphere of 5% CO<sub>2</sub> and 95% air. X-irradiation was performed at 95 kV, 25 mA, and a dose rate of approximately 6 Gy/min, as determined by chemical dosimetry. For the colony formation assay, cells in culture dishes in medium were irradiated at room temperature and plated in two different dilutions in triplicate. Colonies were stained after 7 (K1, AA8, xrs-6, V3, V3-147, and V3-155) or 10 (irs1SF and CXR3) days. For immunofluorescence measurements, cells were irradiated on coverslips immersed in culture medium at room temperature. To chemically inhibit DSB repair by inactivating DNA-PK<sub>cs</sub> (see 30-min time points in Fig. 2B), we incubated cells from 30 min before until 30 min after irradiation in the presence of 200  $\mu$ M phosphatidylinositol 3-kinase inhibitor 2-(4-morpholinyl)-8-phenyl-4H-1-benzopyran-4-one (LY294002) (68). For PFGE measurements, cells were irradiated in flasks filled with ice-cold phosphate-buffered saline (PBS; 137 mM NaCl, 2.7 mM KCl, 8 mM Na<sub>2</sub>HPO<sub>4</sub>, 1.5 mM KH<sub>2</sub>PO<sub>4</sub> [pH 7.45]), which was replaced with prewarmed medium for repair incubation. Control samples were sham irradiated in all experiments.

**Cell synchronization and flow cytometry.** Cells were seeded at a density of  $8 \times 10^4$  per cm<sup>2</sup> and grown for 3 to 4 days to obtain G<sub>1</sub>-phase cells;  $4 \times 10^4$  G<sub>1</sub>-phase cells per cm<sup>2</sup> were grown for 16 h in medium containing 1  $\mu$ g of aphidicolin/ml. Under these conditions, cells accumulate at the G<sub>1</sub>/S border. Then, the aphidicolin-containing medium was removed, and the cells were incubated for 6 h (6.5 h for irs1SF cells) in fresh medium to obtain G<sub>2</sub>-phase cells. Measurements of cell cycle distributions were obtained by using a FACScan flow cytometer (Becton Dickinson). Cells were harvested, resuspended in PBS, fixed with 70% ethanol at -20°C, and stained with propidium iodide-RNase A. Two-parameter (bromodeoxyuridine [BrdU] plus propidium iodide) flow cytometry measurements were obtained by using a BrdU flow kit with fluorescein isothiocyanate-conjugated anti-BrdU antibody (Becton Dickinson). Fluorescence data were plotted by using CellQuest software (Becton Dickinson).

**Immunofluorescence microscopy.** Cells were fixed in 2% paraformaldehyde for 15 min, washed three times in PBS for 10 min each time, permeabilized for 5 min on ice in 0.2% Triton X-100, and blocked three times in PBS with 1% bovine serum albumin for 10 min each time at room temperature. The coverslips were incubated with anti- $\gamma$ -H2AX antibody (Trevigen) for 1 h, washed three times in PBS-1% bovine serum albumin for 10 min each time, and incubated with Alexa Fluor 488-conjugated goat anti-rabbit secondary antibody (Molecular Probes) for 1 h at room temperature. Cells were washed four times in PBS for 10 min each time and mounted by using Vectashield mounting medium with 4,6-

diamidino-2-phenylindole (Vector Laboratories). Fluorescence images were captured by using a Zeiss Axioskop 2mot epifluorescence microscope equipped with a charge-coupled device camera and ISIS software (Metasystems). Optical sections through the nuclei were captured at 0.3- $\mu$ m intervals, and the images were obtained by projection of the individual sections. For quantitative analysis, foci were counted by eye during the microscopic and imaging process by using a  $\times 100$  objective. The error bars in the figures represent the standard error of the mean (SEM) for 40 to 80 cells per sample. BrdU labeling and immunofluorescence detection of BrdU-positive cells were performed by using cell proliferation labeling reagent and monoclonal anti-BrdU antibody (Amersham Pharmacia Biotech), which was detected with Alexa Fluor 594-conjugated goat anti-mouse secondary antibody (Molecular Probes). Cells were treated first with anti- $\gamma$ -H2AX antibody and then with anti-BrdU antibody.

**PFGE.** DSB repair studies were performed as previously described (27, 34, 47). Briefly, cells were harvested, embedded in agarose plugs ( $6 \times 10^5$  cells per plug), and lysed. Electrophoresis was carried out with a CHEF-DR system and agarose gels. The gels were run at 14°C with linearly increasing pulse times from 50 to 5,000 s over 65 h at a field strength of 1.5 V/cm. The gels were stained with ethidium bromide, and the fraction of DNA below the well was quantified with commercially available software. Experiments measuring the fraction of DNA below the well as a function of dose were performed in parallel with repair experiments, and the results served as a calibration to obtain relative numbers of remaining DSBs from the fraction of DNA below the well in the samples used in the repair experiments.

#### RESULTS

**Primarily NHEJ determines DSB repair in the G<sub>1</sub> phase.** In the present study, we investigated the repair of DSBs in synchronized populations of CHO cells defective either in NHEJ or in HR by analyzing  $\gamma$ -H2AX focus formation in situ and DSBs in vitro. Parental AA8 cells, XRCC3-defective irs1SF cells (32), and DNA-PK<sub>cs</sub>-defective V3 cells (23) were grown to confluence to obtain at least 90% G<sub>1</sub>-phase cells (Fig. 1A). Analysis by PFGE of the time course for DSB repair after 80 Gy of irradiation shows that V3 cells have a pronounced repair defect, consistent with previous measurements (48). However, irs1SF cells repair DSBs with kinetics similar to those of AA8 cells (Fig. 1B and C). After a repair period of 24 h, nearly all DSBs are rejoined in both AA8 and irs1SF cells. Notably, no DNA degradation and only slight changes in cell cycle distribution (see irs1SF cell data) occur following 80 Gy of irradiation and repair times of up to 24 h (Fig. 1A).

$\gamma$ -H2AX focus formation was investigated with G<sub>1</sub>-arrested control and 1-Gy-irradiated cultures (Fig. 2). Without irradiation, the numbers of foci per cell were as follows: AA8, 0.2; irs1SF, 0.4; and V3, 1.0. Although IR-induced foci are visible after 15 min of incubation, quantitation in CHO cells is reliable only at later times, when the foci become more distinct (Fig. 2A) (foci in primary human fibroblasts can be quantified 15 min and even 3 min after irradiation; see Discussion). Because DSB repair occurs during the time period necessary for focus formation, we wished to inhibit repair in order to obtain information on the initial numbers of IR-induced foci. Therefore, cells were incubated in the presence of the phosphatidylinositol 3-kinase inhibitor LY294002 (68), which inactivates DNA-PK<sub>cs</sub>. With this approach, all cell lines investigated show the same number of foci per cell ( $n = 30$ ) 30 min after irradiation, demonstrating equal efficiencies in  $\gamma$ -H2AX focus formation (Fig. 2B). The kinetics of the disappearance of foci show a pronounced repair defect for V3 cells compared with parental AA8 and irs1SF cells. Significantly, for all three cell lines, the kinetics of the disappearance of foci resemble the kinetics of DSB repair determined from PFGE analysis after

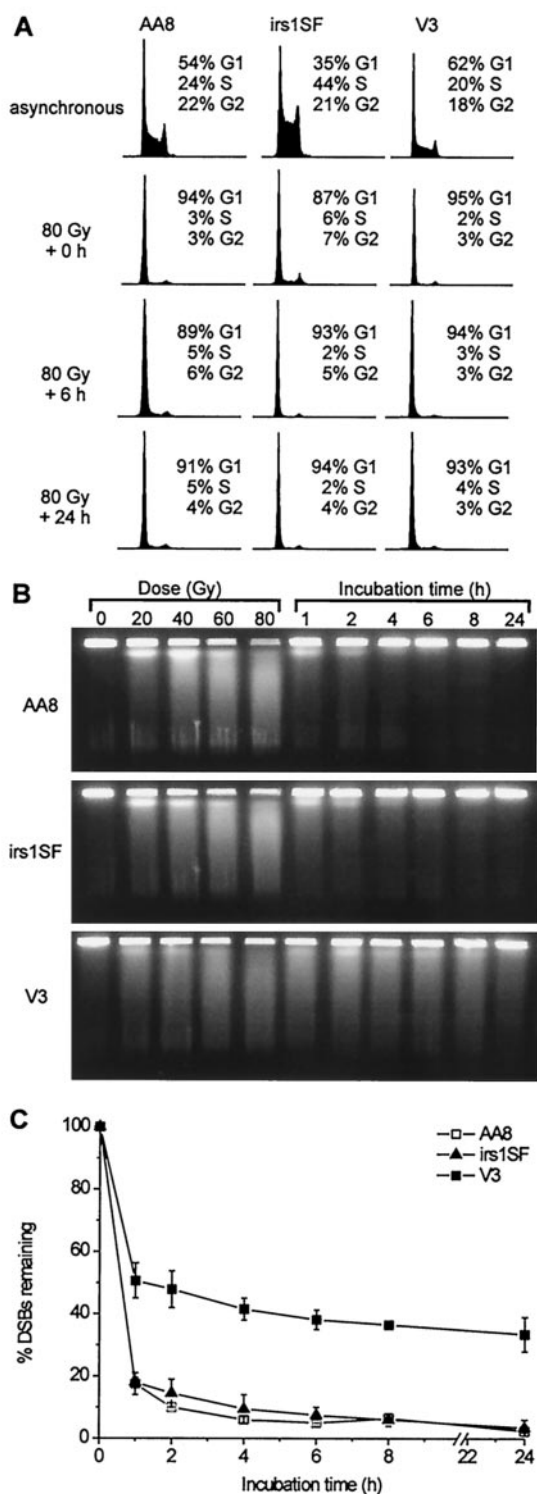


FIG. 1. DSB repair in  $G_1$ -phase cells, as determined by PFGE. (A) DNA histograms for asynchronous cultures (upper row) and  $G_1$ -phase cells at various incubation times after 80 Gy of irradiation (lower rows). (B) Ethidium bromide images of DNA from  $G_1$ -phase cells irradiated with various doses and incubated for repair after 80 Gy of irradiation. (C) Time course for the percentage of initial DSBs remaining after repair. Error bars represent SEMs from two or three experiments.

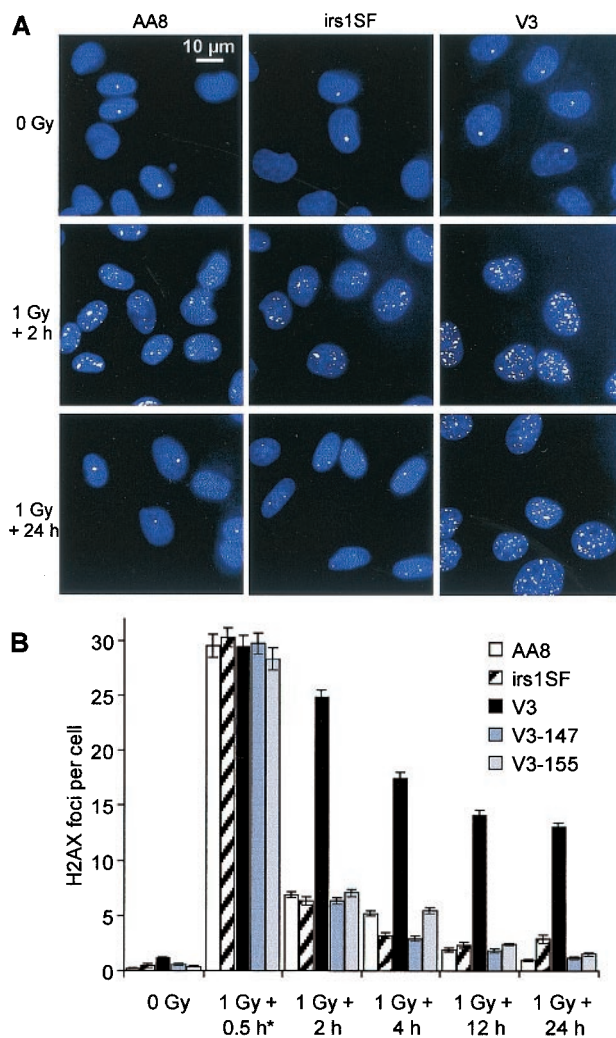


FIG. 2. DSB repair in  $G_1$ -phase cells, as measured by  $\gamma$ -H2AX focus formation. (A)  $\gamma$ -H2AX foci (green) in nonirradiated and irradiated cells; nuclei were stained with 4,6-diamidino-2-phenylindole (blue). (B) Time course for the repair of DSBs after 1 Gy of irradiation. The mean number of foci per cell for various repair times is shown. Numbers of foci in nonirradiated controls were subtracted. The 0.5-h time point (asterisk) was obtained by incubating the cells in the presence of LY294002 to inhibit repair. Error bars represent SEMs.

80 Gy of irradiation (Fig. 2B). This similarity provides further evidence that each  $\gamma$ -H2AX focus directly reflects the presence of a DSB. V3 cells complemented with a yeast artificial chromosome containing either the human (V3-147) (6) or the mouse (V3-155) (39) DNA-PK<sub>cs</sub> gene show a repair capacity similar to that of parental AA8 cells. Moreover, the loss of foci after 1 Gy of irradiation, as contrasted with DSBs at a higher dose, appears incomplete in irs1SF cells 24 h after treatment.

Because V3 and irs1SF cells are radiosensitive in asynchronous populations (17, 59, 72), we wished to compare asynchronous cells to  $G_1$ -phase populations. Cell survival experiments confirm that both NHEJ and HR contribute to the radioresistance of asynchronous cells (Fig. 3A). While V3 and xrs-6 cells show  $\sim$ 6-fold sensitivity (derived from a comparison of the doses that result in 20% survival), irs1SF cells are  $\sim$ 3-fold

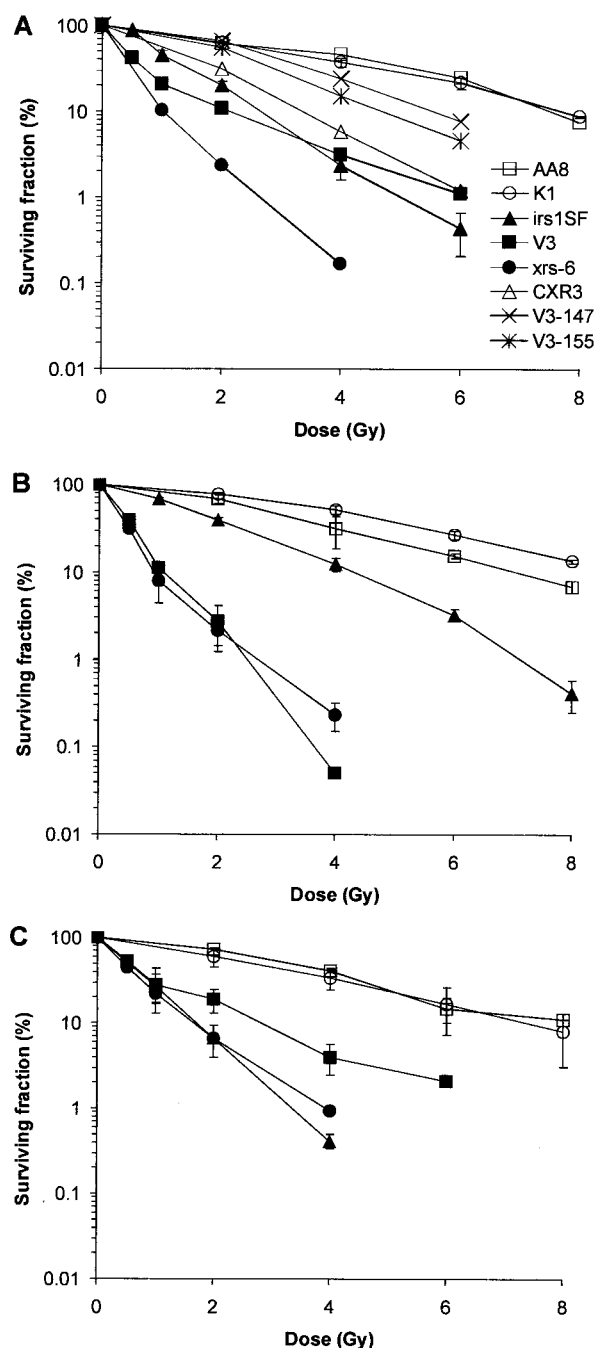


FIG. 3. Radiosensitivity of various CHO cell lines. *xrs-6* is defective in Ku80 and is derived from CHO K1 cells. (A) Asynchronous cells. (B) G<sub>1</sub> phase. (C) Late S/G<sub>2</sub> phase. Error bars represent SEMs from one or two (A) or two or three (B and C) independent experiments.

sensitive. *irs1SF* cells complemented with human *XRCC3* cDNA (CXR3 cells) show only partial correction of radiosensitivity, in agreement with previous results (59). Notably, V3 cells show a pronounced biphasic survival curve, suggesting the presence of a resistant subpopulation. V3 cells complemented with the human or mouse DNA-PK<sub>cs</sub> gene show substantial correction of radiosensitivity. When cell survival in the G<sub>1</sub>

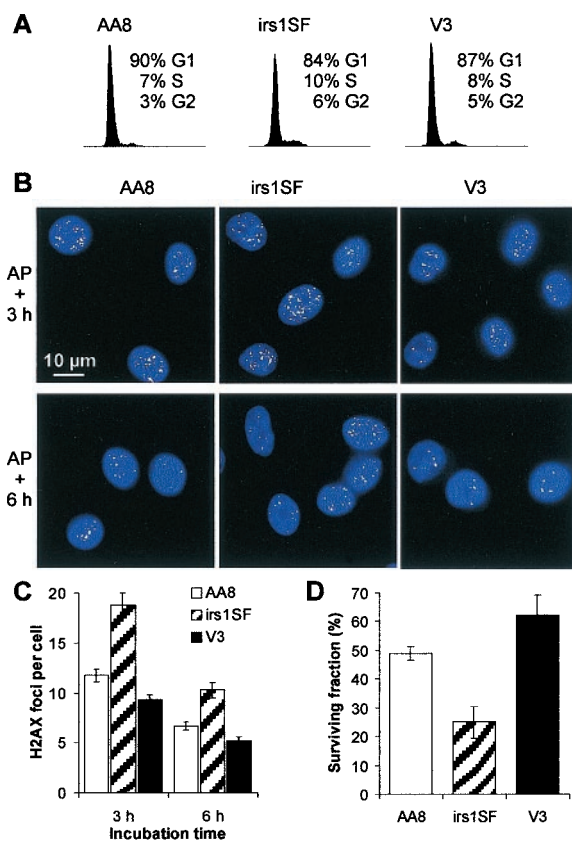


FIG. 4. Effect of aphidicolin on cell cycle arrest,  $\gamma$ -H2AX focus formation, and cell survival. (A) DNA histograms for cells treated for 16 h with aphidicolin. (B)  $\gamma$ -H2AX foci (green) 3 and 6 h (3.5 and 6.5 h for *irs1SF* cells because of their slower growth) after treatment with aphidicolin (AP); nuclei were stained with 4,6-diamidino-2-phenylindole (blue). (C) Mean number of foci per cell after 3 and 6 h (3.5 and 6.5 h for *irs1SF* cells) after aphidicolin treatment. (D) Cell survival after aphidicolin treatment. Error bars represent SEMs.

phase is assessed (Fig. 3B), V3 (but not *xrs-6*) cells show increased sensitivity compared with an asynchronous population. Significantly, compared to AA8 cells, *irs1SF* cells in the G<sub>1</sub> phase are substantially less sensitive (~1.5-fold) than those in the exponential phase. Because surviving cells likely proceed from G<sub>1</sub> into other cell cycle phases while repair occurs, this 1.5-fold sensitivity does not necessarily imply that cells use HR during the G<sub>1</sub> phase. Taken together, the relatively proficient repair in *irs1SF* cells that were arrested in G<sub>1</sub> up to 24 h after IR exposure, as well as the observation that *irs1SF* cells are much more resistant in the G<sub>1</sub> phase than in other phases, suggests that XRCC3-dependent HR plays only a modest role in DSB repair and survival of cells irradiated in G<sub>1</sub>.

**HR determines the repair of replication-associated DSBs induced by aphidicolin.** To investigate the influence of cell cycle position on the choice of DSB repair pathways, we synchronized the cells by treatment with aphidicolin, an inhibitor of replication polymerases. Confluent cells were subcultured and incubated for 16 h in the presence of 1  $\mu$ g of aphidicolin/ml, allowing them to proceed to the beginning of the S phase (Fig. 4A). After the removal of aphidicolin, the cells synchronously proceed into S and G<sub>2</sub> (Fig. 5A). We analyzed aphidi-

colin-induced  $\gamma$ -H2AX focus formation at 3 and 6 h after drug removal (Fig. 4B). Significantly, the number of foci in irs1SF cells was substantially higher than that in V3 or AA8 cells at both times (Fig. 4C). The rate of survival of irs1SF cells was significantly lower than that of V3 or AA8 cells, consistent with the increased number of foci in irs1SF (Fig. 4D). These findings strongly suggest that aphidicolin sensitivity is caused by defective DSB repair occurring through HR. Apparently, NHEJ is not involved in the repair of aphidicolin-induced DSBs, consistent with the idea that “one-sided” DSBs are generated at sites of replication inhibition (12).

**Both NHEJ and HR contribute to IR-induced DSB repair in the late-S/G<sub>2</sub> phase.** We next addressed the contributions of NHEJ and HR in repairing IR-induced DSBs in S and G<sub>2</sub>. At 3 and 6 h after the removal of aphidicolin, when the cultures contained mid-S- and late-S/G<sub>2</sub>-phase cells, respectively (Fig. 5A), 1 Gy of irradiation was delivered. Enumeration of  $\gamma$ -H2AX foci at 2 and 4 h after irradiation in mid-S phase (3 h after aphidicolin removal) revealed that V3 cells were substantially deficient in DSB repair, while irs1SF cells showed a smaller defect (Fig. 5C). These results contrast with those for aphidicolin-induced DSB repair. Thus, HR is used for replication-associated DSB repair but is not, per se, the predominant DSB repair pathway during the S phase. Cells irradiated 6 h after aphidicolin removal were also examined. While nonirradiated cells start to enter mitosis  $\sim$ 7 h after aphidicolin removal (data not shown), 1 Gy of irradiation delays entry into mitosis for at least 2 h (i.e., 8 h after aphidicolin removal). At 4 h after irradiation, most of the AA8 and V3 cells and half of the irs1SF cells have traversed into G<sub>1</sub> (Fig. 5A). While V3 cells now show a repair deficiency comparable to that of cells in the “AP + 3 h” condition, irs1SF cells in late S/G<sub>2</sub> are much more compromised than those in mid-S (Fig. 5D). Thus, the relative importance of HR in repairing IR-induced DSBs increases from G<sub>1</sub> through S and into late S/G<sub>2</sub>. Both HR and NHEJ contribute significantly to IR-related DSB repair in late S/G<sub>2</sub>. These results contrast with those for aphidicolin-induced DSB repair, which depends only on HR. The large number of foci in cells that were irradiated in late S/G<sub>2</sub> and reached G<sub>1</sub> 4 h later (Fig. 5A [bottom row] and Fig. 5D) implies that cells pass through mitosis with many DSBs ( $\geq$ 10). Indeed, cells in mitosis 2 to 4 h after irradiation in late S/G<sub>2</sub> always displayed  $\gamma$ -H2AX foci at the ends of chromosome fragments (Fig. 5E).

The observation that V3 cells show normal repair of aphidicolin-induced DSBs but deficient repair of DSBs induced by IR in mid-S phase demonstrates the different requirements for NHEJ in replication-associated versus radiation-induced DSB repair. However, determining the cell cycle-specific contributions of HR and NHEJ to IR-induced DSB repair (Fig. 5) is limited by the DSBs produced by aphidicolin and the possibility that artificial arrest at the G<sub>1</sub>/S border interferes with normal physiological processes. This limitation is particularly relevant for irs1SF cells, which show, compared with AA8 and V3 cells, defective DSB repair and compromised survival after aphidicolin treatment. Therefore, we investigated the cell cycle dependence of DSB repair in asynchronous populations. Cells were pulse-labeled with BrdU for 30 min (Fig. 6) and irradiated with 1 Gy either immediately or 2 h after BrdU labeling. Following repair times of 2 or 4 h, BrdU-positive cells were analyzed for  $\gamma$ -H2AX focus formation (Fig. 6B and C). BrdU-

positive cells are evenly distributed throughout the S phase at the time of irradiation when irradiation occurs immediately after BrdU labeling; alternatively, they have progressed to late S/G<sub>2</sub> when irradiation occurs 2 h after labeling (Fig. 6A). Results from such an analysis show that DSBs induced in the S phase by radiation are primarily repaired by NHEJ (Fig. 6D), while HR and NHEJ both contribute substantially when DSBs are introduced during late S/G<sub>2</sub> (Fig. 6E). These data are in agreement with the results shown in Fig. 5.

It is noteworthy that nonirradiated BrdU-positive irs1SF cells analyzed 2 or 4 h after BrdU labeling show higher levels of  $\gamma$ -H2AX foci than comparable AA8 or V3 cells. At 2 h after BrdU treatment, the numbers of foci per cell were as follows: irs1SF, 1.3; AA8, 0.4; and V3, 0.5. At 4 h after BrdU treatment, these values were as follows: irs1SF, 1.4; AA8, 0.4; and V3, 0.6. These results are in contrast to those for nonirradiated cells arrested in G<sub>1</sub> (Fig. 2B) but are consistent with the higher level of foci in aphidicolin-treated irs1SF cells compared with V3 cells (Fig. 4C). Perhaps related to this finding is the significantly higher S-phase fraction of exponentially growing irs1SF cells compared with AA8 and V3 cells that is observed after BrdU labeling (Fig. 6B; irs1SF, 36% BrdU-positive cells; AA8, 29%; and V3, 20%) and by flow cytometry (Fig. 1A [top row]; irs1SF, 44% S-phase DNA; AA8, 24%; and V3, 20%), as well as the reduced rate of growth of irs1SF cells (59). These observations are consistent with a role of HR in repairing DSBs that arise spontaneously during replication (19, 54), leading to more DSBs in irs1SF cells after replication and to a higher S-phase fraction associated with retarded S-phase traversal and slower growth.

To evaluate whether the contributions of HR and NHEJ to the repair of IR-induced DSBs are reflected in radiosensitivity measurements, we determined the survival rates for late-S/G<sub>2</sub>-phase cells by irradiating and plating the cells 6 h after removing aphidicolin. In contrast to the radiosensitivity seen with asynchronous and G<sub>1</sub>-phase cell populations, the HR and NHEJ mutants show similar sensitivities ( $\sim$ 6-fold for xrs-6 and irs1SF cells but  $\sim$ 3-fold for V3 cells) (Fig. 3C). Compared to the G<sub>1</sub>-phase results (Fig. 3B), these findings represent for the NHEJ mutants similar (xrs-6 cells) or somewhat reduced (V3 cells) sensitivity, versus a dramatically increased sensitivity for the HR mutants (6-fold in late S/G<sub>2</sub> versus 1.5-fold in G<sub>1</sub>). These observations agree with the DSB repair data in supporting the idea that NHEJ is important for survival after IR in all phases of the cell cycle, while HR primarily contributes to radioresistance in the late-S/G<sub>2</sub> phase. However, HR does contribute to the resistance of cells irradiated in the G<sub>1</sub>/early-S phase.

## DISCUSSION

**$\gamma$ -H2AX foci provide a measure of DSB repair after physiologically relevant IR doses.** Here we used  $\gamma$ -H2AX focus formation to quantify the repair of IR-induced DSBs. Initial studies showed a close relationship between the number of  $\gamma$ -H2AX foci and the number of expected DSBs after treatment with IR (46). Recently, a direct correlation was observed between the number of foci and the number of DSBs produced by decay of <sup>125</sup>I incorporated into cellular DNA (51), suggesting that each focus represents an individual break and that

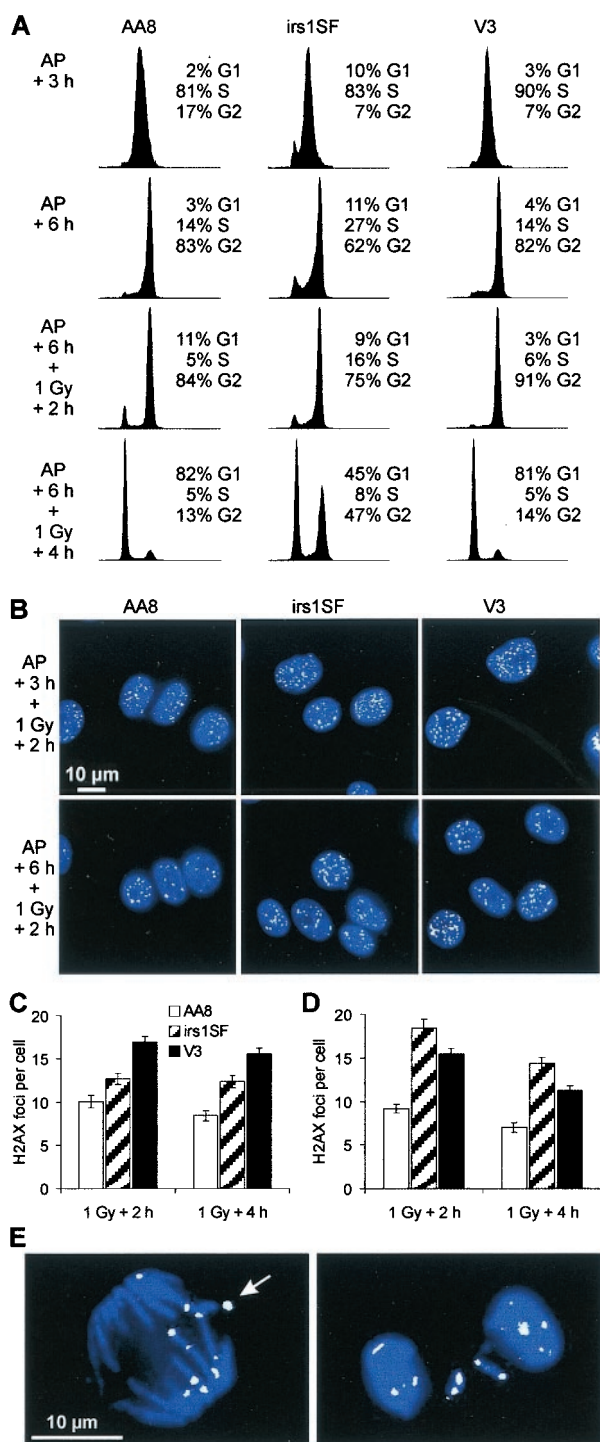


FIG. 5. DSB repair in S and G<sub>2</sub>-phase cells, as measured by  $\gamma$ -H2AX focus formation. (A) DNA histograms either 3 h (first row; 3.5 h for irs1SF cells) and 6 h (second row; 6.5 h for irs1SF cells) after aphidicolin (AP) removal or 2 h (third row) and 4 h (fourth row) after 1 Gy of irradiation given at 6 or 6.5 h after aphidicolin removal. (B)  $\gamma$ -H2AX foci (green) 2 h after 1 Gy of irradiation at 3 or 3.5 h (upper row) and 6 or 6.5 h (lower row) after aphidicolin removal; nuclei were stained with 4,6-diamidino-2-phenylindole (blue). (C) Mean number of foci per cell 2 and 4 h after 1 Gy of irradiation at 3 or 3.5 h after aphidicolin removal. (D) Mean number of foci per cell 2 and 4 h after 1 Gy of irradiation at 6 or 6.5 h after aphidicolin removal. Error bars represent SEMs. (E)  $\gamma$ -H2AX foci (green) in

each DSB forms a focus. However, the relationship between DSB repair and the disappearance of  $\gamma$ -H2AX foci is less clear. Our PFGE data in Fig. 1C show that ~40% of the 80-Gy-induced DSBs in V3 cells are not repaired at 4 to 24 h after irradiation; these data are similar to the  $\gamma$ -H2AX focus measurements in G<sub>1</sub>-phase V3 cells (Fig. 2B). Importantly, G<sub>1</sub>-phase HR-defective irs1SF cells had almost normal DSB repair kinetics for both  $\gamma$ -H2AX and PFGE end points. Further evidence that  $\gamma$ -H2AX foci are a valid measure not only of DSB formation but also of repair comes from other recent studies. In our laboratory, the induction and repair of IR-induced DSBs in primary human fibroblasts in the G<sub>1</sub> phase were studied by examining  $\gamma$ -H2AX focus formation in parallel with PFGE assays (49). Initial yields of DSBs induced by doses between 10 and 80 Gy were determined with a specialized PFGE assay (33, 43) and compared to the number of foci detected 3 min after irradiation with 2 Gy or less. We observed essentially the same number of DSBs, 35 per Gy per cell, measured at a high dose, as we did of the number of foci per gray per cell, measured at  $\leq 2$  Gy. The value of 30 initial DSBs per Gy per CHO cell reported in this study (Fig. 2B) is consistent with 35 initial DSBs per Gy per human fibroblast, as flow cytometry analysis showed that primary human fibroblasts contain approximately 20% more DNA than CHO cells (data not shown). In the same study of Rothkamm and Löbrich (49), the kinetics of the disappearance of foci closely resembled the kinetics of DSB repair, for both repair-proficient and DNA ligase IV-defective primary human fibroblasts.

**HR and NHEJ differentially contribute to IR-induced DSB repair during the cell cycle.** By using  $\gamma$ -H2AX focus analysis as an approach for DSB repair measurements, Rothkamm and Löbrich conducted the first study of DSB repair in mammalian cells by using physiologically relevant radiation doses (49). A second major advantage of the  $\gamma$ -H2AX approach is its applicability to repair measurements in the S phase, where PFGE is compromised due to electrophoresis artifacts resulting from structural abnormalities of replicating DNA. Our results show that NHEJ is the predominant repair pathway not only in the G<sub>1</sub> phase but also, surprisingly, is more important than XRCC3-dependent HR for the repair of DSBs introduced by IR during most of the S phase (Fig. 5C and 6D). However, both HR and NHEJ contribute significantly to the repair of DSBs produced by IR during the late-S/G<sub>2</sub> phase (Fig. 5D and 6E). This finding is the first direct demonstration of a contribution of HR to the repair of IR-induced DSBs. The results of the  $\gamma$ -H2AX experiments are consistent with survival measurements, which show that HR-defective cells are most sensitive in late S/G<sub>2</sub> and only modestly sensitive in G<sub>1</sub>. In contrast, NHEJ-deficient cells show pronounced sensitivity throughout the cell cycle but are slightly more resistant in late S/G<sub>2</sub> than in G<sub>1</sub> (Fig. 3). These observations can be summarized in a model (Fig. 7) in which NHEJ contributes substantially to DSB repair and radioresistance in all cell cycle phases, while HR contrib-

mitotic AA8 cells between 2 and 4 h after 1 Gy of irradiation at 6 h after aphidicolin removal; DNA was stained with 4,6-diamidino-2-phenylindole (blue). The  $\gamma$ -H2AX focus indicated by the arrow coincides with a small chromosomal fragment that was invisible due to the superposition of the blue and the green images.

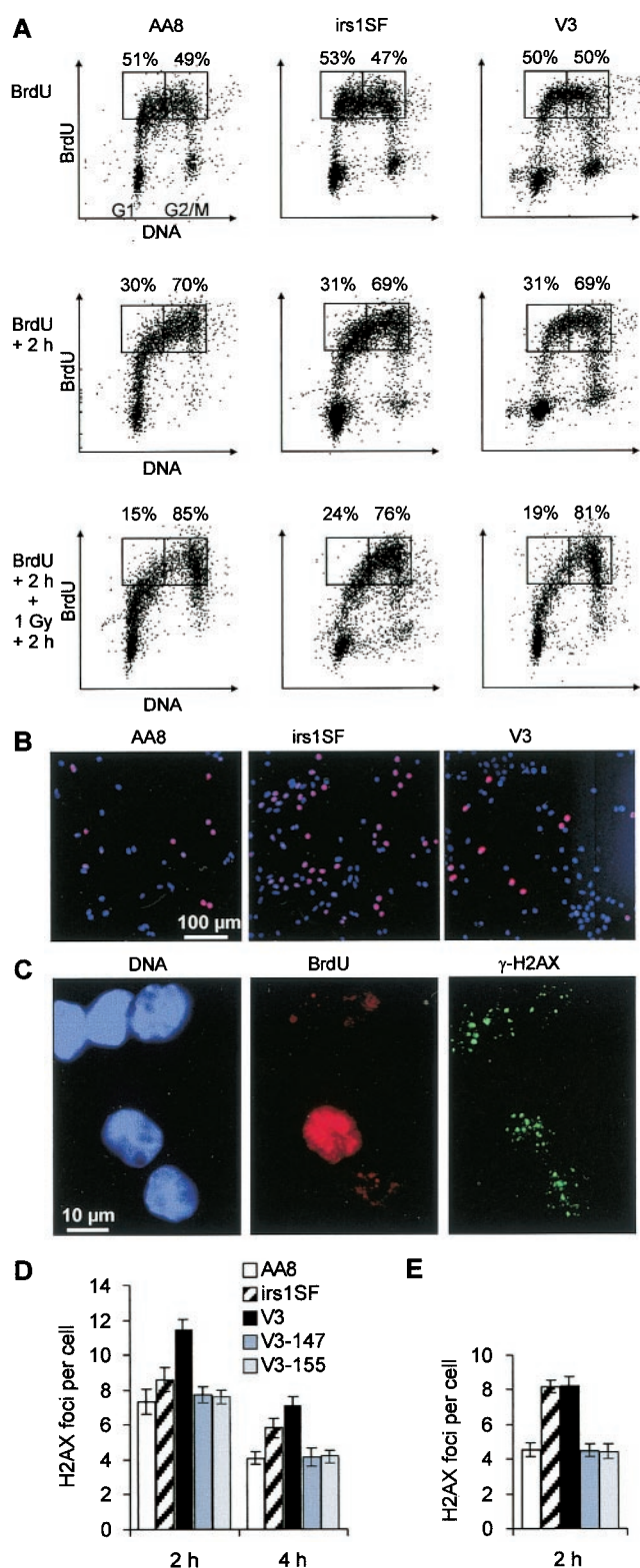


FIG. 6. DSB repair in BrdU-positive cells, as measured by  $\gamma$ -H2AX focus formation. (A) Two-parameter (propidium iodide and BrdU) flow cytometry diagrams of asynchronous cultures of AA8, irs1SF, and V3 cells either immediately (upper row) or 2 h (middle row) after 30 min of pulse-labeling with BrdU or 2 h after 1 Gy of irradiation at 2 h after BrdU labeling (lower row). The numbers above the rectangles in each diagram refer to the proportions of BrdU-positive cells with a

utes modestly in G<sub>1</sub> and progressively more as cells move through the cycle into G<sub>2</sub>.

The absolute percent contribution of each pathway cannot be determined from these experiments because irs1SF cells are incompletely defective in HR. Although homology-directed repair of I-SceI-produced DSBs strongly depends on XRCC3 (7, 38), the level of spontaneous chromosomal aberrations is considerably lower in *xrcc3* than in conditionally deficient *rad51* DT40 chicken cells (54, 58). Additionally, a basal level of HR is essential for the viability of mouse and chicken cells (30, 54). These results suggest that Rad51 has a more important role than XRCC3 for the repair of spontaneous DSBs. It is therefore possible that IR-induced DSBs also are repaired by an HR process that depends only partly on XRCC3. Because spontaneous DSBs likely arise during replication, while restriction enzymes can produce DSBs in all cell cycle phases, we cannot exclude the possibility that the XRCC3 requirement of HR varies throughout the cell cycle. Thus, the full quantitative contribution of HR to DSB repair throughout the cell cycle could be considerably greater than that suggested by the phenotype of irs1SF cells. Moreover, some end joining still occurs in the absence of DNA-PK (62, 63).

It is unlikely that the contribution of HR to DSB repair and survival of cells irradiated in G<sub>1</sub> results from recombination occurring between homologous chromosomes in G<sub>1</sub>. In mouse embryonic stem cells, the homolog-dependent repair of enzymatically induced DSBs occurs at a low frequency,  $\sim 3 \times 10^{-6}$  (41). Moreover, the karyotype of CHO cells is highly rearranged, a fact which might further reduce the likelihood of pairing and recombination between homologous alleles. We suggest that the increased sensitivity of *xrcc3* mutant cells to irradiation in the G<sub>1</sub> phase can be explained by DSB repair occurring during the S phase. For example, DSBs that arise in G<sub>1</sub> and that become replicated might be repaired by a two-step process in which NHEJ rejoins one chromatid, thereby providing a substrate by which HR could repair the other chromatid. Thus, NHEJ and HR could cooperate to increase the efficiency of repair.

Our observations showing that HR is involved in the repair of radiation-induced DSBs when the sister chromatid is available as an information donor are consistent with cell survival and chromosome aberration measurements obtained with DT40 chicken cells (57, 58). Studies with CHO cells in which DSBs were generated enzymatically in chromosomally integrated HR substrates showed that repair occurs predominantly by gene conversion with the sister chromatid as a template (25). This HR process is greatly reduced (by 25- to 250-fold) in

DNA content either lower or higher than that of mid-S-phase cells. (B) Asynchronous cultures of AA8, irs1SF, and V3 cells after 30 min of pulse-labeling with BrdU (red); nuclei were stained with 4,6-diamidino-2-phenylindole (blue). (C)  $\gamma$ -H2AX foci (green) in AA8 cells 2 h after 1 Gy of irradiation immediately after BrdU labeling (red); nuclei were stained with 4,6-diamidino-2-phenylindole (blue). (D) Mean number of foci per BrdU-positive cell 2 and 4 h after 1 Gy of irradiation immediately after BrdU labeling. (E) Mean number of foci per BrdU-positive cell 2 h after 1 Gy of irradiation at 2 h after BrdU labeling. Numbers of foci in nonirradiated controls were subtracted. Error bars represent SEMs. Results obtained from a second independent set of experiments with AA8, irs1SF, and V3 cells were nearly identical to the data shown in panels D and E.

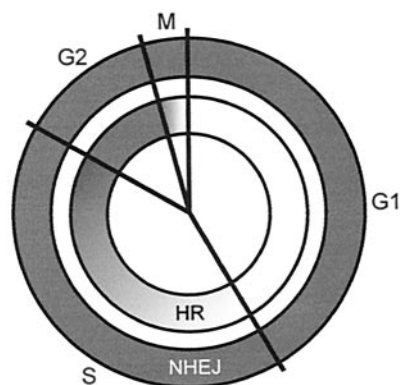


FIG. 7. Model of the relative contributions of HR and NHEJ to the repair of IR-induced DSBs in different cell cycle phases, based on mutant phenotypes. Whereas NHEJ predominates in  $G_1$ /early S, both HR and NHEJ contribute substantially to DSB repair during late S/ $G_2$ .

irs1SF cells (7, 38). Also, irs1SF cells show high levels of spontaneous (59) and IR-induced chromosomal aberrations, a defect that could be corrected by complementing the cells with human chromosome 14, which contains the *XRCC3* gene (13).

Earlier studies with synchronized populations of NHEJ-deficient cells reported an increased efficiency of IR-induced DSB repair in late S/ $G_2$  compared with  $G_1$ , suggesting the operation of an HR pathway in late S/ $G_2$  (29, 36). However, measurements with HR-defective cells repeatedly failed to display a DSB repair defect in physical assays (2, 10, 17, 26, 60, 70). Because those studies were performed at IR doses of  $>20$  Gy, it is likely that the burden of DSBs ( $>600$  per cell) prohibited the detection of the contribution of HR. Although those studies were performed with asynchronous cultures, in analogous experiments, we did not observe a repair defect in irs1SF cells synchronized in late S/ $G_2$  with aphidicolin (I. Krüger et al., unpublished data). These findings suggest that HR is saturated at high IR doses, with the vast majority of DSBs being repaired by NHEJ in late S/ $G_2$ . The data presented here clearly show the necessity of using physiologically relevant IR doses to measure the contribution of HR.

**HR repairs DNA replication-associated DSBs.** We have shown that aphidicolin treatment produces  $\gamma$ -H2AX foci, which disappear more slowly in irs1SF cells than in wild-type and V3 cells after drug removal. Because cell survival after aphidicolin treatment is also reduced the most in irs1SF cells, it appears that aphidicolin-induced DSBs are primarily repaired by HR. DSBs arising from replication fork blockage after UV irradiation result in  $\gamma$ -H2AX focus formation (31, 71), and PFGE measurements show that aphidicolin induces DSBs specifically during the S phase (50). However, the genetic requirements for the repair of replication-associated DSBs are still poorly defined. While some authors have reported a pronounced sensitivity of NHEJ-deficient cells (50), others have observed a cytotoxic effect of replication inhibitors primarily in cells defective in HR (1, 35). Some of these discrepancies may well be related to the use of different replication inhibitors, but there is clearly a need to study the interplay between replication and repair by using an assay that directly quantifies DSBs and their repair at biologically relevant doses.

Our data argue that aphidicolin-induced replication-associated DSBs are exclusively repaired by HR, whereas IR-induced DSBs in the S phase are primarily repaired by NHEJ, with a lesser contribution of HR. Since most endogenous DSBs are thought to be replication associated and since HR is much less likely than NHEJ to cause genomic rearrangements (42), these findings may have important implications for evaluating radiation risk compared to risk from endogenous DNA damage.

#### ACKNOWLEDGMENTS

We thank P. Jeggo for kindly providing AA8, V3, and DNA-PK<sub>cs</sub>-complemented V3 cells and R. Greinert for providing K1 cells; xrs-6 cells (European Collection of Cell Cultures) are commercially available.

Financial support was provided by the Deutsche Forschungsgemeinschaft (grants Lo 677/1-1 and Lo 677/1-2), the Radiation Protection Programme of the European Community (grant FIGH-CT-1999-00012), and the Bundesministerium für Bildung und Forschung via the Forschungszentrum Karlsruhe (grant 02S8132). A portion of this work was prepared under the auspices of the U.S. Department of Energy by Lawrence Livermore National Laboratory under contract no. W-7405-ENG-48 and was funded by the Low-Dose Radiation Research Program, Biological and Environmental Research, U.S. Department of Energy (grant SCW0389/0008).

#### REFERENCES

1. Arnaudeau, C., C. Lundin, and T. Helleday. 2001. DNA double-strand breaks associated with replication forks are predominantly repaired by homologous recombination involving an exchange mechanism in mammalian cells. *J. Mol. Biol.* **307**:1235–1245.
2. Asaad, N. A., Z. C. Zeng, J. Guan, J. Thacker, and G. Iliakis. 2000. Homologous recombination as a potential target for caffeine radiosensitization in mammalian cells: reduced caffeine radiosensitization in XRCC2 and XRCC3 mutants. *Oncogene* **19**:5788–5800.
3. Baumann, P., and S. C. West. 1997. The human Rad51 protein: polarity of strand transfer and stimulation by hRP-A. *EMBO J.* **16**:5198–5206.
4. Baumann, P., and S. C. West. 1998. Role of the human RAD51 protein in homologous recombination and double-stranded-break repair. *Trends Biochem. Sci.* **23**:247–251.
5. Bezzubova, O., A. Silbergleit, Y. Yamaguchi-Iwai, S. Takeda, and J. M. Buerstedde. 1997. Reduced X-ray resistance and homologous recombination frequencies in a RAD54<sup>-/-</sup> mutant of the chicken DT40 cell line. *Cell* **89**:185–193.
6. Blunt, T., N. J. Finnie, G. E. Taccioli, G. C. Smith, J. Demengeot, T. M. Gottlieb, R. Mizuta, A. J. Varghese, F. W. Alt, P. A. Jeggo, and S. P. Jackson. 1995. Defective DNA-dependent protein kinase activity is linked to V(D)J recombination and DNA repair defects associated with the murine scid mutation. *Cell* **80**:813–823.
7. Brenneman, M. A., A. E. Weiss, J. A. Nickoloff, and D. J. Chen. 2000. XRCC3 is required for efficient repair of chromosome breaks by homologous recombination. *Mutat. Res.* **459**:89–97.
8. Cartwright, R., C. E. Tambini, P. J. Simpson, and J. Thacker. 1998. The XRCC2 DNA repair gene from human and mouse encodes a novel member of the recA/RAD51 family. *Nucleic Acids Res.* **26**:3084–3089.
9. Chang, C., K. A. Biedermann, M. Mezzina, and J. M. Brown. 1993. Characterization of the DNA double strand break repair defect in scid mice. *Cancer Res.* **53**:1244–1248.
10. Cheong, N., Y. Wang, M. Jackson, and G. Iliakis. 1992. Radiation-sensitive irs mutants rejoin DNA double-strand breaks with efficiency similar to that of parental V79 cells but show altered response to radiation-induced G2 delay. *Mutat. Res.* **274**:111–122.
11. Cheong, N., X. Wang, Y. Wang, and G. Iliakis. 1994. Loss of S-phase-dependent radioresistance in irs-1 cells exposed to X-rays. *Mutat. Res.* **314**:77–85.
12. Cromie, G. A., J. C. Connelly, and D. R. F. Leach. 2001. Recombination at double-strand breaks and DNA ends: conserved mechanisms from phage to humans. *Mol. Cell* **8**:1163–1174.
13. Cui, X., M. Brenneman, J. Meyne, M. Oshimura, E. H. Goodwin, and D. J. Chen. 1999. The XRCC2 and XRCC3 repair genes are required for chromosome stability in mammalian cells. *Mutat. Res.* **434**:75–88.
14. Dronkert, M. L., H. B. Beverloo, R. D. Johnson, J. H. Hoeijmakers, M. Jasin, and R. Kanaar. 2000. Mouse RAD54 affects DNA double-strand break repair and sister chromatid exchange. *Mol. Cell. Biol.* **20**:3147–3156.
15. Essers, J., R. W. Hendriks, S. M. Swagemakers, C. Troelstra, J. de Wit, D. Bootsma, J. H. Hoeijmakers, and R. Kanaar. 1997. Disruption of mouse RAD54 reduces ionizing radiation resistance and homologous recombination. *Cell* **89**:195–204.



16. Essers, J., H. van Steeg, J. de Wit, S. M. Swagemakers, M. Vermeij, J. H. Hoeijmakers, and R. Kanaar. 2000. Homologous and non-homologous recombination differentially affect DNA damage repair in mice. *EMBO J.* **19**:1703–1710.
17. Fuller, L. F., and R. B. Painter. 1988. A Chinese hamster ovary line hypersensitive to ionizing radiation and deficient in repair replication. *Mutat. Res.* **193**:109–121.
18. Golub, E. I., R. C. Gupta, T. Haaf, M. S. Wold, and C. M. Radding. 1998. Interaction of human rad51 recombination protein with single-stranded DNA binding protein, RPA. *Nucleic Acids Res.* **26**:5388–5393.
19. Haber, J. E. 1999. DNA recombination: the replication connection. *Trends Biochem. Sci.* **24**:271–275.
20. Haber, J. E. 2000. Partners and pathways repairing a double-strand break. *Trends Genet.* **16**:259–264.
21. Hoeijmakers, J. H. 2001. Genome maintenance mechanisms for preventing cancer. *Nature* **411**:366–374.
22. Jackson, S. P. 2002. Sensing and repairing DNA double-strand breaks. *Carcinogenesis* **23**:687–696.
23. Jeggo, P. A. 1998. DNA breakage and repair. *Adv. Genet.* **38**:185–218.
24. Johnson, R. D., N. Liu, and M. Jasin. 1999. Mammalian XRCC2 promotes the repair of DNA double-strand breaks by homologous recombination. *Nature* **401**:397–399.
25. Johnson, R. D., and M. Jasin. 2000. Sister chromatid gene conversion is a prominent double-strand break repair pathway in mammalian cells. *EMBO J.* **19**:3398–3407.
26. Jones, N. J., S. A. Stewart, and L. H. Thompson. 1990. Biochemical and genetic analysis of the Chinese hamster mutants *irs1* and *irs2* and their comparison to cultured ataxia telangiectasia cells. *Mutagenesis* **5**:15–23.
27. Kühne, M., K. Rothkamm, and M. Löbrich. 2000. No dose-dependence of DNA double-strand break misrejoining following alpha-particle irradiation. *Int. J. Radiat. Biol.* **76**:891–900.
28. Kurimasa, A., S. Kumano, N. V. Boubnov, M. D. Story, C. S. Tung, S. R. Peterson, and D. J. Chen. 1999. Requirement for the kinase activity of human DNA-dependent protein kinase catalytic subunit in DNA strand break rejoining. *Mol. Cell. Biol.* **19**:3877–3884.
29. Lee, S. E., R. A. Mitchell, A. Cheng, and E. A. Hendrickson. 1997. Evidence for DNA-PK-dependent and -independent DNA double-strand break repair pathways in mammalian cells as a function of the cell cycle. *Mol. Cell. Biol.* **17**:1425–1433.
30. Lim, D. S., and P. Hasty. 1996. A mutation in mouse *rad51* results in an early embryonic lethal that is suppressed by a mutation in *p53*. *Mol. Cell. Biol.* **16**:7133–7143.
31. Limoli, C. L., E. Giedzinski, W. M. Bonner, and J. E. Cleaver. 2002. UV-induced replication arrest in the xeroderma pigmentosum variant leads to DNA double-strand breaks, gamma-H2AX formation, and Mre11 relocation. *Proc. Natl. Acad. Sci. USA* **99**:233–238.
32. Liu, N., J. E. Lamerdin, R. S. Tebbs, D. Schild, J. D. Tucker, M. R. Shen, K. W. Brookman, M. J. Siciliano, C. A. Walter, W. Fan, L. S. Narayana, Z. Q. Zhou, A. W. Adamson, K. J. Sorensen, D. J. Chen, N. J. Jones, and L. H. Thompson. 1998. XRCC2 and XRCC3, new human Rad51-family members, promote chromosome stability and protect against DNA cross-links and other damages. *Mol. Cell* **1**:783–793.
33. Löbrich, M., B. Rydberg, and P. K. Cooper. 1995. Repair of x-ray-induced DNA double-strand breaks in specific *NorI* restriction fragments in human fibroblasts: joining of correct and incorrect ends. *Proc. Natl. Acad. Sci. USA* **92**:12050–12054.
34. Löbrich, M., M. Kühne, J. Wetzel, and K. Rothkamm. 2000. Joining of correct and incorrect DNA double-strand break ends in normal human and ataxia telangiectasia fibroblasts. *Genes Chromosomes Cancer* **27**:59–68.
35. Lundin, C., K. Erixon, C. Arnaudeau, N. Schultz, D. Jansen, M. Meuth, and T. Helleday. 2002. Different roles for nonhomologous end joining and homologous recombination following replication arrest in mammalian cells. *Mol. Cell. Biol.* **22**:5869–5878.
36. Mateos, S., P. Slijepcevic, R. A. MacLeod, and P. E. Bryant. 1994. DNA double-strand break rejoining in *xrs5* cells is more rapid in the G2 than in the G1 phase of the cell cycle. *Mutat. Res.* **315**:181–187.
37. Olive, P. L. 1998. The role of DNA single- and double-strand breaks in cell killing by ionizing radiation. *Radiat. Res.* **150**:S42–S51.
38. Pierce, A. J., R. D. Johnson, L. H. Thompson, and M. Jasin. 1999. XRCC3 promotes homology-directed repair of DNA damage in mammalian cells. *Genes Dev.* **13**:2633–2638.
39. Priestley, A., H. J. Beamish, D. Gell, A. G. Amatucci, M. C. Muhlmann-Diaz, B. K. Singleton, G. C. Smith, T. Blunt, L. C. Schalkwyk, J. S. Bedford, S. P. Jackson, P. A. Jeggo, and G. E. Taccioli. 1998. Molecular and biochemical characterisation of DNA-dependent protein kinase-defective rodent mutant *irs-20*. *Nucleic Acids Res.* **26**:1965–1973.
40. Riballo, E., S. E. Critchlow, S. H. Teo, A. J. Doherty, A. Priestley, B. Broughton, B. Kysela, H. Beamish, N. Plovman, C. F. Arlett, A. R. Lehmann, S. P. Jackson, and P. A. Jeggo. 1999. Identification of a defect in DNA ligase IV in a radiosensitive leukaemia patient. *Curr. Biol.* **9**:699–702.
41. Richardson, C., M. E. Moynahan, and M. Jasin. 1998. Double-strand break repair by interchromosomal recombination: suppression of chromosomal translocations. *Genes Dev.* **12**:3831–3842.
42. Richardson, C., and M. Jasin. 2000. Frequent chromosomal translocations induced by DNA double-strand breaks. *Nature* **405**:697–700.
43. Rief, N., and M. Löbrich. 2002. Efficient rejoining of radiation-induced DNA double-strand breaks in centromeric DNA of human cells. *J. Biol. Chem.* **277**:20572–20582.
44. Rijkers, T., J. Van Den Ouweland, B. Morolli, A. G. Rolink, W. M. Baarends, P. P. Van Sloun, P. H. Lohman, and A. Pastink. 1998. Targeted inactivation of mouse RAD52 reduces homologous recombination but not resistance to ionizing radiation. *Mol. Cell. Biol.* **18**:6423–6429.
45. Rogakou, E. P., D. R. Pilch, A. H. Orr, V. S. Ivanova, and W. M. Bonner. 1998. DNA double-stranded breaks induce histone H2AX phosphorylation on serine 139. *J. Biol. Chem.* **273**:5858–5868.
46. Rogakou, E. P., C. Boon, C. Redon, and W. M. Bonner. 1999. Megabase chromatin domains involved in DNA double-strand breaks in vivo. *J. Cell Biol.* **146**:905–916.
47. Rothkamm, K., and M. Löbrich. 1999. Misrejoining of DNA double-strand breaks in primary and transformed human and rodent cells: a comparison between the HPRT region and other genomic locations. *Mutat. Res.* **433**:193–205.
48. Rothkamm, K., M. Kühne, P. A. Jeggo, and M. Löbrich. 2001. Radiation-induced genomic rearrangements formed by nonhomologous end-joining of DNA double-strand breaks. *Cancer Res.* **61**:3886–3893.
49. Rothkamm, K., and M. Löbrich. 2003. Evidence for a lack of DNA double-strand break repair in human cells exposed to very low x-ray doses. *Proc. Natl. Acad. Sci. USA* **100**:5057–5062.
50. Saintigny, Y., F. Delacote, G. Vares, F. Petitot, S. Lambert, D. Averbeck, and B. S. Lopez. 2001. Characterization of homologous recombination induced by replication inhibition in mammalian cells. *EMBO J.* **20**:3861–3870.
51. Sedelnikova, O. A., E. P. Rogakou, I. G. Panyutin, and W. M. Bonner. 2002. Quantitative detection of (125)IdU-induced DNA double-strand breaks with gamma-H2AX antibody. *Radiat. Res.* **158**:486–492.
52. Sigurdsson, S., K. Trujillo, B. Song, S. Stratton, and P. Sung. 2001. Basis for avid homologous DNA strand exchange by human Rad51 and RPA. *J. Biol. Chem.* **276**:8798–8806.
53. Smith, G. C., and S. P. Jackson. 1999. The DNA-dependent protein kinase. *Genes Dev.* **13**:916–934.
54. Sonoda, E., M. S. Sasaki, J. M. Buerstedde, O. Bezzubova, A. Shinohara, H. Ogawa, M. Takata, Y. Yamaguchi-Iwai, and S. Takeda. 1998. Rad51-deficient vertebrate cells accumulate chromosomal breaks prior to cell death. *EMBO J.* **17**:598–608.
55. Stamato, T. D., R. Weinstein, A. Giaccia, and L. Mackenzie. 1983. Isolation of cell cycle-dependent gamma ray-sensitive Chinese hamster ovary cell. *Somatic Cell Genet.* **9**:165–173.
56. Sung, P., K. M. Trujillo, and S. Van Komen. 2000. Recombination factors of *Saccharomyces cerevisiae*. *Mutat. Res.* **451**:257–275.
57. Takata, M., M. S. Sasaki, E. Sonoda, C. Morrison, M. Hashimoto, H. Utsumi, Y. Yamaguchi-Iwai, A. Shinohara, and S. Takeda. 1998. Homologous recombination and non-homologous end-joining pathways of DNA double-strand break repair have overlapping roles in the maintenance of chromosomal integrity in vertebrate cells. *EMBO J.* **17**:5497–5508.
58. Takata, M., M. S. Sasaki, S. Tachiiri, T. Fukushima, E. Sonoda, D. Schild, L. H. Thompson, and S. Takeda. 2001. Chromosome instability and defective recombinational repair in knockout mutants of the five Rad51 paralogs. *Mol. Cell. Biol.* **21**:2858–2866.
59. Tebbs, R. S., Y. Zhao, J. D. Tucker, J. B. Scheerer, M. J. Siciliano, M. Hwang, N. Liu, R. J. Legerski, and L. H. Thompson. 1995. Correction of chromosomal instability and sensitivity to diverse mutagens by a cloned cDNA of the XRCC3 DNA repair gene. *Proc. Natl. Acad. Sci. USA* **92**:6354–6358.
60. Thacker, J., and A. N. Ganesh. 1990. DNA-break repair, radioresistance of DNA synthesis, and camptothecin sensitivity in the radiation-sensitive *irs* mutants: comparisons to ataxia-telangiectasia cells. *Mutat. Res.* **235**:49–58.
61. Thacker, J. 1999. A surfeit of RAD51-like genes? *Trends Genet.* **15**:166–168.
62. Thompson, L. H., and D. Schild. 1999. The contribution of homologous recombination in preserving genome integrity in mammalian cells. *Biochimie* **81**:87–105.
63. Thompson, L. H., and D. Schild. 2001. Homologous recombinational repair of DNA ensures mammalian chromosome stability. *Mutat. Res.* **477**:131–153.
64. Thompson, L. H., and D. Schild. 2002. Recombinational DNA repair and human disease. *Mutat. Res.* **509**:49–78.
65. Tucker, J. D., N. J. Jones, N. A. Allen, J. L. Minkler, L. H. Thompson, and A. V. Carrano. 1991. Cytogenetic characterization of the ionizing radiation-sensitive Chinese hamster mutant *irs1*. *Mutat. Res.* **254**:143–152.
66. Van Dyck, E., A. Z. Stasiak, A. Stasiak, and S. C. West. 1999. Binding of double-strand breaks in DNA by human Rad52 protein. *Nature* **398**:728–731.
67. van Gent, D. C., J. H. Hoeijmakers, and R. Kanaar. 2001. Chromosomal stability and the DNA double-stranded break connection. *Nat. Rev. Genet.* **2**:196–206.

68. **Vlahos, C. J., W. F. Matter, K. Y. Hui, and R. F. Brown.** 1994. A specific inhibitor of phosphatidylinositol 3-kinase, 2-(4-morpholinyl)-8-phenyl-4H-1-benzopyran-4-one (LY294002). *J. Biol. Chem.* **269**:5241–5248.
69. **Wachsberger, P. R., W. H. Li, M. Guo, D. Chen, N. Cheong, C. C. Ling, G. Li, and G. Iliakis.** 1999. Rejoining of DNA double-strand breaks in Ku80-deficient mouse fibroblasts. *Radiat. Res.* **151**:398–407.
70. **Wang, H., Z. C. Zeng, T. A. Bui, E. Sonoda, M. Takata, S. Takeda, and G. Iliakis.** 2001. Efficient rejoining of radiation-induced DNA double-strand breaks in vertebrate cells deficient in genes of the RAD52 epistasis group. *Oncogene* **20**:2212–2224.
71. **Ward, I. M., and J. Chen.** 2001. Histone H2AX is phosphorylated in an ATR-dependent manner in response to replicational stress. *J. Biol. Chem.* **276**:47759–47762.
72. **Whitmore, G. F., A. J. Varghese, and S. Gulyas.** 1989. Cell cycle responses of two X-ray sensitive mutants defective in DNA repair. *Int. J. Radiat. Biol.* **56**:657–665.
73. **Yamaguchi-Iwai, Y., E. Sonoda, J. M. Buerstedde, O. Bezzubova, C. Morrison, M. Takata, A. Shinohara, and S. Takeda.** 1998. Homologous recombination, but not DNA repair, is reduced in vertebrate cells deficient in RAD52. *Mol. Cell. Biol.* **18**:6430–6435.